

LASER FREQUENCY STANDARDS https://doi.org/10.1070/QEL17134

Magic wavelengths near 800 nm for precision spectroscopy of an inner-shell transition in thulium atoms

D.O. Tregubov, A.A. Golovizin, E.S. Fedorova, K.Yu. Khabarova, V.N. Sorokin, N.N. Kolachevsky

Abstract. **Differential dynamic polarisability of the inner-shell clock transition at a wavelength of 1.14 μm in the thulium atom is measured by the method of precision laser spectroscopy in the spectral range of 800–860 nm. Experimental data approximated by a theoretical model yield the probability of the transition at $\lambda = 809.5$ nm: $A_{809.5} = 460(70)\,s^{-1}$. The values of two magic wavelengths are obtained experimentally, namely, $\lambda_{m1} = 807.727(18)$ nm and $\lambda_{m2} = 813.3(2)$ nm, the wavelength of λ_{m1} being determined for the first time. Main parameters of an optical lattice at these wavelengths are compared and a conclusion is made that trapping thulium atoms in an optical lattice at λ_{m2} is preferable for optical clock operation.**

Keywords: *polarisability, magic wavelength, optical clock, clock transition, ultra cold atoms, thulium.*

1. Introduction

High accuracy of optical frequency references gives a chance to perform unique experiments aimed at studying a possible drift of fundamental physical constants, testing general theory of relativity, searching for dark matter and so on [1–3]. Sensitivity of the transition frequency to gravity potential opens possibilities to draw maps of the Earth gravitation field, which requires a high-accuracy transportable optical clock [4]. The limiting characteristics of optical frequency references can be obtained by either controlling the heat environment of atoms with a high accuracy [5–7], or using cryogenic systems [8, 9], or searching for systems insensitive to thermal radiation [10–12].

Inner-shell transitions in some atoms of lanthanide group possess a low sensitivity to thermal radiation. Earlier, we have shown [13] that a relative frequency shift at a temperature of 300 K for the inner-shell clock transition 1.14 μm in the thulium atom is as low as $2.3(1.1) \times 10^{-18}$; thus, there is no need to stabilise the temperature of the environment.

The sensitivity of the transition frequency to thermal radiation and external electrical fields is determined by its differential polarisability. The method for calculating a differential polarisability described in [14–16] is based on using the values of energy and probability for all transitions from lower or upper levels of the clock transition (including transitions to continuum). This approach is also used for preliminary estimation of the magic wavelengths for clock transitions at which the differential dynamic polarisability turns to zero. A calculation error depends on the accuracy of determining energies of known transitions, their probabilities and some other factors. Trapping atoms in an optical lattice at a magic wavelength provides precision spectroscopy of a clock transition and makes it possible to realise an optical clock with a relative uncertainty reaching 10^{-18} [6, 17].

Calculations performed by our group [14] have shown that in the range of 800–860 nm, one may expect at least one magic wavelength for the inner-shell transition in the thulium atom. Indeed, measurements performed [13] succeeded in finding the magic wavelength equal to 813.320(6) nm. Its existence and position are mainly determined by a near-lying transition from the upper clock level $|4f^{13}(^2F^o)6s^2;\ J = 5/2\rangle \rightarrow |4f^{12}(^3F_4)5d_{3/2}6s^2;\ J = 7/2\rangle$ at a wavelength of 809.5 nm. In the present work, a spectrum of the differential polarisability is recorded for clock levels, and its improved theoretical model in the wavelength range of 800–860 nm is developed. By using the suggested model, characteristics were determined of the transition $|4f^{13}(^2F^o)6s^2;\ J = 5/2\rangle \rightarrow |4f^{12}(^3F_4)5d_{3/2}6s^2;\ J = 7/2\rangle$ at a wavelength of 809.5 nm which has not been studied yet. The position of one more magic wavelength in this range was found and compared to the previously determined magic wavelength.

2. Model of the spectrum of differential dynamic polarisability

The energy level diagram of the thulium atom, which determines the spectrum of differential polarisability in the range of 800–860 nm, is shown in Fig. 1. Atomic energy levels shift in the presence of an external electromagnetic radiation due to the Stark effect. As a result, the frequency of the transition between levels $|F, J, m_F\rangle \rightarrow |F', J', m_F'\rangle$ changes according to the formula

$$\Delta\nu = -\frac{2\pi a_0^3}{hc}[\alpha_{J',F',m_F'} - \alpha_{J,F,m_F}]I_{\text{eff}}, \qquad (1)$$

where a_0 is the Bohr radius; h is the Planck constant; c is the speed of light; I_{eff} is the radiation intensity; and α_{J,F,m_F} is the dynamic polarisability of the level $|J, F, m_F\rangle$ in atomic units (here, J is the angular momentum of the electron shell, F is the total angular momentum of the atom, and m_F is the projection of the total angular momentum). In this

D.O. Tregubov, A.A. Golovizin Lebedev Physical Institute, Russian Academy of Sciences, Leninsky prosp. 53, 119991 Moscow, Russia; e-mail: treg.dim@gmail.com;
E.S. Fedorova, K.Yu. Khabarova, V.N. Sorokin, N.N. Kolachevsky Lebedev Physical Institute, Russian Academy of Sciences, Leninsky prosp. 53, 119991 Moscow, Russia; Russian Quantum Centre, Skolkovo IC, Bolshoi bulvar 30, stroenie 1, 121205 Moscow, Russia

Received 16 September 2019; revision received 27 September 2019
Kvantovaya Elektronika **49** (11) 1028–1031 (2019)
Translated by N.A. Raspopov

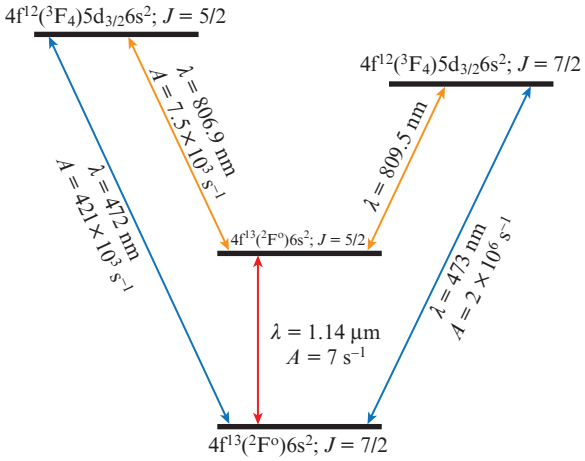

Figure 1. Energy levels of thulium atoms, which mainly determine a spectrum of differential dynamic polarisability in the range 800–815 nm. All the transition probabilities are taken from papers [18, 25]. Hyperfine level splitting is not shown.

case, $\Delta\alpha = \alpha_{J',F',m'_F} - \alpha_{J,F,m_F}$ is the differential dynamic polarisability of the transition. In the present paper, we use atomic units for polarisability: 1 a.u. $= 4\pi\varepsilon_0 a_0^3$.

The polarisability of the atomic level α_{J,F,m_F} in the linearly polarised electromagnetic field comprises scalar α_J^{S} and tensor α_J^{T} components [16]:

$$\alpha_{J,F,m_F} = \alpha_J^{\mathrm{S}} + \frac{3\cos^2\theta - 1}{2}\,\frac{3m_F^2 - F(F+1)}{F(2F-1)}\,\alpha_{J,F}^{\mathrm{T}}, \tag{2}$$

$$\alpha_{J,F}^{\mathrm{T}} = \alpha_J^{\mathrm{T}}(-1)^{I+J+F}\begin{Bmatrix} J & J & 2 \\ F & F & I \end{Bmatrix} \times \frac{F(2F-1)(2F+1)(2J+3)(2J+1)(J+1)}{(2F+3)(F+1)(2J-1)J}, \tag{3}$$

where the curly brackets denote Wigner's 6-j symbol; θ is the angle between light radiation polarisation and the quantisation axis; and I is the atom nuclear spin.

The scalar and tensor polarisabilities are found from the sum over all possible transitions from the level studied (hereinafter, the studied level is one of fine sublevels of the ground state):

$$\alpha_{J,F}^{\mathrm{T}} = \sum_k \alpha_{J\to J_k} 6(2J+1)(-1)^{J+J_k}\begin{Bmatrix} 1 & 1 & 2 \\ J & J & J_k \end{Bmatrix} \times \sqrt{\frac{5J(2J-1)}{6(J+1)(2J+1)(2J+3)}}, \tag{4}$$

$$\alpha_J^{\mathrm{S}} = \sum_k \alpha_{J\to J_k}, \tag{5}$$

$$\alpha_{J\to J_k} = \frac{c^3}{2a_0^3}\,\frac{2J_k+1}{2J+1}\,\frac{A_k}{\omega_k^2(\omega_k^2-\omega^2)}, \tag{6}$$

where J_k is the moment of an electron shell for the level k; A_k is the probability for a transition between the studied and kth levels; ω_k is the circular frequency of the transition; and ω is the circular frequency of a light source.

Tabulated experimental data for the parameters A_k are incomplete [18]; hence, in polarisability calculations we need theoretical estimates for the transition probabilities. In particular, as far as the clock transition in the thulium atom $|4f^{13}(^2F^o)6s^2;\ J = 7/2,\ F = 4,\ m_F = 0\rangle \to |4f^{13}(^2F^o)6s^2;\ J = 5/2,\ F = 3,\ m_F = 0\rangle$ is concerned, among many transitions in the region of interest $\lambda > 800$ nm, experimental data are available only for the transition at 806.9 nm possessing the probability of $7.5(1.1)\times 10^3$ s^{-1} [19, 20]. Theoretical estimates of transition probabilities were obtained by using Cowan's atomic structure code [14, 21]. In turn, it was shown [14] that the contributions into a continuous spectrum of transitions from both of the clock levels are rather close and do not substantially affect a value of the differential polarisability.

3. Experiment

For determining the differential dynamic polarisability, thulium atoms are prepared at a temperature of about 10 μK. An atomic cloud is cooled by the method of double-stage laser cooling [22] with the following recapturing of atoms into a one-dimensional vertical optical lattice trap inside an enhancement cavity at a certain wavelength [23]. The radiation power P inside the cavity is measured by a calibrated photodiode placed behind the outcoupling mirror with a known transmission coefficient (Fig. 2), whereas the beam waist radius $w = 126$ μm is determined by the cavity geometry. In experiments, the radiation power inside the cavity varied from 1 to 3 W, which corresponds to the antinode intensity of 16–42 kW cm^{-2} (a depth of the trap in temperature units is 6.5–20 μK).

Thus, intensity $I_{\mathrm{eff}} = 8\eta P/(\pi w^2)$ included in (1) is related to the lattice antinode intensity by the coefficient $\eta \leqslant 1$. Atoms in the lattice have non-zero temperature and fill several vibrational levels, which reduces the radiation intensity accepted by atoms. In our experiments, the polarisation of the optical lattice emission coincides with a direction of the magnetic field, which defines the quantisation axis (Fig. 2). The laser

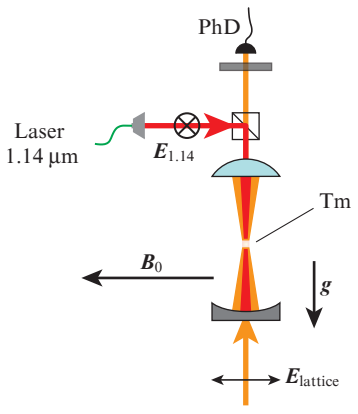

Figure 2. Schematic of an experiment on determining the differential polarisability of the clock transition:
($\boldsymbol{B}_0$) magnetic field, which determines a quantisation axis; (Ph D) photodiode for measuring the lattice emission power; ($\boldsymbol{E}_{\mathrm{lattice}}$) and ($\boldsymbol{E}_{1.14}$) polarisation vectors for the optical lattice and for radiation at 1.14 μm, respectively; (Tm) position of the atomic cloud in the lattice. The radiation of a Ti : sapphire laser, which forms the optical lattice, passes from below.

radiation used for exciting the clock transition is adjusted in resonance with the transition between sublevels $|F = 4, m_F = 0\rangle \rightarrow |F' = 3, m'_F = 0\rangle$, and its frequency can be scanned by an acousto-optical modulator for measuring a transition excitation profile. The contrast of an absorption spectrum is increased by optically pumping the sublevel $|F = 4, m_F = 0\rangle$ [24]. Precision spectroscopy of atoms trapped in the lattice by using a narrow-band laser at a wavelength of 1.14 μm makes it possible to measure the frequency shift of a clock transition caused by an optical lattice. This shift turns out to be proportional to the differential dynamic polarisability of radiation:

$$\Delta\nu = -\frac{16\eta a_0^3}{hcw^2}\Delta\alpha P. \qquad (7)$$

According to calculations [14], magic wavelengths are expected in the range of 800–815 nm. An optical lattice was formed by the radiation of a Ti:sapphire laser, which wavelength varied in the range of 800–860 nm. Thus, the entire search range of magic wavelengths was covered, which made it possible then to approximate data accurately.

While developing a model for approximation of experimental data, in (4) one can select two kinds of summands depending on the resonance and nonresonance character in the wavelength range in question. The first group includes contributions of transitions from the clock level with wavelengths 806.9 and 809.5 nm (the corresponding electron configuration and other parameters are presented in Fig. 1). A contribution of probabilities for other transitions into the differential polarisability $A(\omega)$ weakly depends on the wavelength in the considered range and varies from –0.269 to –0.270 a.u. [14]. Thus, experimental data were approximated by using the model:

$$\Delta\alpha = \frac{\Delta\nu}{P}\frac{hcw^2}{16\eta a_0^3} = \frac{c^3}{a_0^3}\left[6.152\frac{A_{806.9}}{\omega_{806.9}^2(\omega_{806.9}^2 - \omega^2)} + 8.048\frac{A_{809.5}}{\omega_{809.5}^2(\omega_{809.5}^2 - \omega^2)}\right] + A(\omega) + \alpha_0. \qquad (8)$$

Expression (8) comprises three free parameters: unknown transition probability $A_{809.5}$, the coefficient η, which characterises an effective field intensity of the lattice, and shift α_0 independent of frequency, which is related to inaccuracy of calculation of a contribution from nonresonance transitions. In experiments, we have chosen the polarisation of the optical lattice corresponding to $\theta = 0$ in (2), and detected the shift of the hyperfine component $|F = 4, m_F = 0\rangle \rightarrow |F' = 3, m'_F = 0\rangle$ of the clock transition. Coefficients at summands in expression (8) were calculated from formulae (2)–(6).

The approximation yielded the following parameter values:

$$\eta = 0.68(9),$$

$$A_{809.5} = 460(70)\ \text{s}^{-1}, \qquad (9)$$

$$\alpha_0 = -0.11(6)\ \text{a.u.}$$

The transition probability $A_{806.9} = 7.5(1.1) \times 10^3\ \text{s}^{-1}$ measured earlier in [20] introduces the main error into approximation parameters. Correctness of the model is confirmed by the reduced parameter $\chi^2 = 1.8$, which is close to unity. The value of parameter η agrees with the theoretical estimate made in [13] $\eta = 0.76(15)$. A small value of α_0 comparable with the error confirms correctness of the theoretically calculated contribution from other atomic transitions into the differential polarisability.

4. Results

Figure 3 shows two domains where the differential polarisability $\Delta\alpha$ turns to zero, which corresponds to magic wavelengths. By using the model approximation described above one can determine the values of the latter, namely, $\lambda_{m1} = 807.727(18)$ nm and $\lambda_{m2} = 813.3(2)$ nm. Importantly, the value found for λ_{m2} coincides with that obtained in [13] within the experimental error. The lower accuracy of the found λ_{m2} in this case relates to the employment of the model for differential polarisability of clock levels in a wide range 800–860 nm, whereas the value in [13] was measured in the immediate vicinity of this wavelength. The corresponding derivatives for the approximation function at the magic wavelengths are $d\alpha/d\lambda|_{m1} = -1.39(20)$ a.u. nm^{-1} and $d\alpha/d\lambda|_{m2} = -0.087(12)$ a.u. nm^{-1}. The measurement error of a magic wavelength is mainly determined by the corresponding derivative and the error in α_0 in (8). Since both the magic wavelengths fit the operation range of Ti:sapphire or semiconductor lasers, it is necessary to compare prospects for their employment in optical clock development.

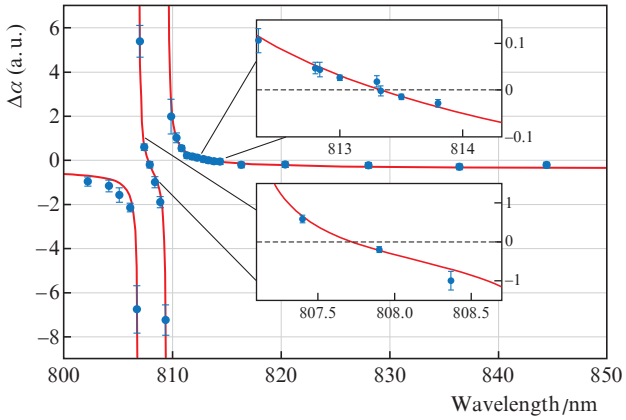

Figure 3. Spectrum of the differential dynamic polarisability of the clock transition [dots refer to experimental data, solid curves correspond to the approximation by model (8)]. Domains near the magic wavelengths are presented in the insets in a large scale.

The derivative $d\alpha/d\lambda|_{m2}$ is approximately 16 times less than $d\alpha/d\lambda|_{m1}$, which softens requirements for the accuracy of laser frequency stabilisation system for an optical lattice. Obtaining the relative frequency instability of a clock transition at a level of 5×10^{-18} in an optical lattice with the intensity $I_{\text{eff}} = 45$ kW cm^{-2} (the lattice depth in this case in the units of recoil energy is 300 E_{recoil}) requires the accuracy of adjusting to λ_{m2} of about 3 MHz. For λ_{m1}, the laser frequency should be stabilised more accurately at a level of 200 kHz, which substantially complicates the problem and requires additional technical solutions.

In turn, the tensor component of the differential dynamic polarisability included in (1) and (2) is seven times less for the

magic wavelength λ_{m2} than for λ_{m1}. Hence, in the case of equal accuracy of adjusting the angle of optical lattice polarisation, the corresponding contribution into the frequency error of a clock transition in under operation at λ_{m2} will be lower by an order of magnitude.

The detuning from nearest resonance transitions affects the rate of optical lattice photon scattering on atoms and atom heating. The rate of scattering can be estimated by using the formula from [14, 16]:

$$\Gamma(\omega)_{0\to 0} = I_{\text{eff}} \frac{6\pi^2 c^2}{h} \sum_k \frac{\omega_k^2 + \omega^2}{(\omega_k^2 - \omega^2)^2} \frac{A_k \Gamma_k}{\omega_k^3} \times (2F_k + 1) \begin{pmatrix} F_k & 1 & F \\ 0 & 0 & 0 \end{pmatrix}^2, \quad (10)$$

where Γ_k is the rate of spontaneous decay for the level k (for example, the values of $\Gamma_{806.9}$ and $\Gamma_{809.5}$ are determined by the decay to the fundamental level as one can see from Fig. 1), brackets denote Wigner's 3-j symbol. For a rate of scattering photons of the optical lattice that has the intensity of 45 kW cm^{-2} from the upper level of the clock transition we have $\Gamma(\lambda_{m1}) \approx \Gamma(\lambda_{m2}) \approx 0.1$ s^{-1}. Note that the transitions 806.9 and 809.5 nm are sufficiently far from both the magic wavelengths and have small probabilities. Hence, those make a small contribution into the scattering rate: approximately only 5% and 0.7% of the total decay value for λ_{m1} and λ_{m2}, respectively. However, proximity of these resonances affects the contribution of hyperpolarisability into a frequency shift of the clock transition. Estimates performed in [14] show that the contributions of hyperpolarisability for the optical lattice with an intensity of 45 kW cm^{-2} are less than 1 Hz and 10 mHz for magic wavelengths λ_{m1} and λ_{m2}, respectively.

Thus, we can unambiguously conclude that the employment of the wavelength $\lambda_{m2} = 813.3$ nm will provide obtaining a higher operation accuracy of an optical clock on thulium atoms.

5. Conclusions

A spectrum of differential dynamic polarisability of the clock transition 1.14 μm in the thulium atom is recorded in the wavelength range of 800–860 nm. The two magic wavelengths are found at $\lambda_{m1} = 807.727(18)$ nm and $\lambda_{m2} = 813.3(2)$ nm, the wavelength λ_{m1} being determined for the first time. The probability of the transition $|4f^{13}(^2F^o)6s^2;\ J = 5/2\rangle \to |4f^{12}(^3F_4)5d_{3/2}6s^2;\ J = 7/2\rangle$ from the upper clock level is determined by using the model developed. A comparison of the two magic wavelengths shows that the employment of λ_{m2} in an optical clock is preferable because at this operation point, the optical clock is less sensitive to a wavelength of the optical lattice and to angle of polarisation of optical lattice emission relative to the magnetic field direction; the value of hyperpolarisability is also less.

It is shown that by using the optical lattice at the wavelength $\lambda_{m2} = 813.3$ nm one can control the relative shifts of a clock transition related to the optical lattice with an accuracy better than 10^{-17}. Works on creation of an optical clock based on the inner-shell transition in the thulium atom are underway in laboratories of Lebedev Physical Institute.

Acknowledgements. The work was supported by the Russian Science Foundation (Grant No. 19-12-00137).

References

1. Ludlow A.D., Boyd M.M., Ye J., Peik E., Schmidt P.O. *Rev. Mod. Phys.*, **87** (2), 637 (2015).
2. Safronova M.S., Porsev S.G., Sanner C., Ye J. *Phys. Rev. Lett.*, **20** (17), 173001 (2018).
3. Derevianko A., Pospelov M. *Nat. Phys.*, **10** (12), 933 (2014).
4. Grotti J., Koller S., Vogt S., Häfner S., Sterr U., Lisdat C., Denker H., Voigt C., Timmen L., Rolland A., et al. *Nat. Phys.*, **14** (5), 437 (2018).
5. Falke S., Lemke N., Grebing C., Lipphardt B., Weyers S., Gerginov V., Huntemann N., Hagemann C., Al-Masoudi A., Häfner S., et al. *New J. Phys.*, **16** (7), 073023 (2014).
6. Bloom B.J., Nicholson T.L., Williams J.R., Campbell S.L., Bishof M., Zhang X., Zhang W., Bromley S.L., Ye J. *Nature*, **506** (7486), 71 (2014).
7. Beloy K., Hinkley N., Phillips N.B., Sherman J.A., Schioppo M., Lehman J., Feldman A., Hanssen L.M., Oates C.W., Ludlow A.D. *Phys. Rev. Lett.*, **113** (26), 260801 (2014).
8. Ushijima I., Takamoto M., Das M., Ohkubo T., Katori H. *Nat. Photonics*, **9** (3), 185 (2015).
9. Middelmann T., Lisdat C., Falke S., Winfred J.S.R.V., Riehle F., Sterr U. *IEEE Trans. Instrum. Meas.*, **60** (7), 2550 (2011).
10. Derevianko A., Dzuba V.A., Flambaum V.V. *Phys. Rev. Lett.*, **109** (18), 180801 (2012).
11. Campbell C.J., Radnaev A.G., Kuzmich A., Dzuba V.A., Flambaum V.V., Derevianko A. *Phys. Rev. Lett.*, **108** (12), 120802 (2012).
12. Yudin V.I., Taichenachev A.V., Okhapkin M.V., Bagayev S.N., Tamm C., Peik E., Huntemann N., Mehlstäubler T.E., Riehle F. *Phys. Rev. Lett.*, **107** (3), 030801 (2011).
13. Golovizin A., Fedorova E., Tregubov D., Sukachev D., Khabarova K., Sorokin V., Kolachevsky N. *Nat. Commun.*, **10** (1), 1724 (2019).
14. Sukachev D., Fedorov S., Tolstikhina I., Tregubov D., Kalganova E., Vishnyakova G., Golovizin A., Kolachevsky N., Khabarova K., Sorokin V. *Phys. Rev. A*, **94** (2), 022512 (2016).
15. Porsev S.G., Ludlow A.D., Boyd M.M., Ye J. *Phys. Rev. A*, **78**, 032508 (2008).
16. Lepers M., Wyart J.-F., Dulieu O. *Phys. Rev. A*, **89**, 022505 (2014).
17. Hinkley N., Sherman J.A., Phillips N.B., Schioppo M., Lemke N.D., Beloy K., Pizzocaro M., Oates C.W., Ludlow A.D. *Science*, **341** (6151), 1215 (2013).
18. Kramida A., Ralchenko Yu., Reader J., NIST ASD Team. https://physics.nist.gov/asd [2019, September 2].
19. Sugar J., Meggers W.F., Camus P. *J. Res. Nat. Bur. Stand. A*, **77** (1), 1 (1973).
20. Wickliffe M.E., Lawler J.E. *J. Opt. Soc. Am B*, **14** (4), 737 (1997).
21. Cowan R.D. *The Theory of Atomic Structure and Spectra, Number 3* (San Diego: Univ. California Press, 1981).
22. Sukachev D.D., Kalganova E.S., Sokolov A.V., Fedorov S.A., Vishnyakova G.A., Akimov A.V., Kolachevsky N.N., Sorokin V.N. *Quantum Electron.*, **44** (6), 515 (2014) [*Kvantovaya Elektron.*, **44** (6), 515 (2014)].
23. Kalganova E.S., Golovizin A.A., Shevnin D.O., Tregubov D.O., Khabarova K.Yu., Sorokin V.N., Kolachevsky N.N. *Quantum Electron.*, **48** (5), 415 (2018) [*Kvantovaya Elektron.*, **48** (5), 415 (2018)].
24. Fedorova E.S., Tregubov D.O., Golovizin A.A., Vishnyakova G.A., Mishin D.A., Rovodchenko D.I., Khabarova K.Yu., Sorokin V.N., Kolachevsky N.N. *Quantum Electron.*, **49** (5), 418 (2019) [*Kvantovaya Elektron.*, **49** (5), 418 (2019)].
25. Kolachevsky N., Akimov A., Tolstikhina I., Chebakov K., Sokolov A., Rodionov P., Kanorski S., Sorokin V. *Appl. Phys. B*, **89** (4), 589 (2007).